Published in final edited form as:
ACS Chem Biol. 2011 October 21; 6(10): 1021–1028. doi:10.1021/cb2002413.

Chemoproteomics-based design of potent LRRK2-selective lead compounds that attenuate Parkinson's disease-related toxicity in human neurons

Nigel Ramsden[b,2,3], **Jessica Perrin**[a,3], **Zhao Ren**[c], **Byoung Dae Lee**[d], **Nico Zinn**[a], **Valina L. Dawson**[d], **Danny Tam**[c], **Michael Bova**[c], **Manja Delling**[a], **Gerard Drewes**[a], **Marcus Bantscheff**[a], **Frederique Bard**[c], **Ted M. Dawson**[d], and **Carsten Hopf**[a,1]

[a] Cellzome AG, Department of Discovery Technology, Meyerhofstrasse 1, D-69117 Heidelberg, Germany

[b] Cellzome Ltd., Department of Drug Discovery, Chesterford Research Park, Cambridge CB10 1XL, United Kingdom

[c] Elan Corporation PLC, 800 Gateway Boulevard, South San Francisco, CA 94080

[d] Johns Hopkins University School of Medicine, Institute for Cell Engineering, Neuroregeneration and Stem Cell Programs, 733 N Broadway, Baltimore, MD 21205

Abstract

Leucine-rich repeat kinase-2 (LRRK2) mutations are the most important cause of familial Parkinson's disease and non-selective inhibitors are protective in rodent disease models. Due to their poor potency and selectivity, the neuroprotective mechanism of these tool compounds has remained elusive so far and it is still unknown whether selective LRRK2 inhibition can attenuate mutant LRRK2-dependent toxicity in human neurons. Here, we employ a chemoproteomics strategy to identify potent, selective and metabolically stable LRRK2 inhibitors. We demonstrate that CZC-25146 prevents mutant LRRK2-induced injury of cultured rodent and human neurons with mid-nanomolar potency. These precise chemical probes further validate this emerging therapeutic strategy. They will enable more detailed studies of LRRK2-dependent signaling and pathogenesis and accelerate drug discovery.

[1] Correspondence should be addressed to C.H. (carsten.hopf@cellzome.com), see address a above, phone ++49 6221 13757-100, FAX ++49 6221 13757-210. [2] Compound requests should go to N.R. (nigel.ramsden@cellzome.com).
[3]These authors contributed equally to the publication

Conflict of interest statement:
B.D.L., V.L.D. and T.M.D. declare no competing financial interests. All other authors declare competing financial interests: **Declaration for authors with affiliations a-c**: These authors are employees of Cellzome AG, Cellzome Ltd or Elan Corporation PLC. These companies funded the work of their respective employees.

AUTHOR CONTRIBUTIONS
N.R. designed and synthesized compounds; J.P. developed the la-S7 assay, conducted the screen and performed protein biochemistry experiments; Z.R., D.T. and M.Bo. performed TR-FRET assays and all experiments in human primary neurons; B.Y.L. performed all experiments in primary rodent neurons. N.Z. and M.L. prepared peptide samples and operated mass spectrometers; N.Z., C.H. and M.Ba. analyzed chemical proteomics data; V.L.D., T.M.D., F.B., M.Ba. and C.H. analyzed data, planned and supervised experiments, N.R. and C.H. conceptualized the project; G.D. contributed ideas and supported the work; and C.H. wrote the paper.

Supporting Information Available:
Additional methods, synthetic procedures, supporting figures, tables and data sets. This material is available free of charge *via* the Internet at http://pubs.acs.org.

Keywords

Chemical Proteomics; Drug Discovery; LRRK2; Parkinson's disease; Neurodegeneration; Sunitinib

Parkinson's disease is a common, debilitating neurodegenerative disease with no established therapy that targets the underlying molecular mechanisms of disease. Mutations in the protein kinase LRRK2 are associated with rare forms of autosomal dominant Parkinson's disease and patients carrying LRRK2 mutations present with symptoms resembling idiopathic Parkinson's disease[1, 2]. Mutations inside (e.g. G2019S) and outside (e.g. R1441C) the kinase domain influence kinase activity and are linked to LRRK2-induced toxicity *in vitro*[3]. *In vivo*, overexpression of wild type LRRK2 alone does not cause neurodegeneration, but it greatly exacerbates the progression of neuropathological abnormalities observed in Parkinson's Disease-related A53T alpha-synuclein transgenic mice[4]. Several inhibitors that display activity against LRRK2 but also against many other kinases have been identified[5-8]. Brain-penetrant, non-selective kinase inhibitors such as GW-5074 are protective in rodent models of LRRK2-induced neurodegeneration *in vitro* and *in vivo,* suggesting that LRRK2 inhibition could be a new treatment paradigm for Parkinson's disease[7]. However, the poor kinase selectivity of GW-5074 and its low potency towards LRRK2 raised the question of whether LRRK2 inhibition alone confers the observed neuroprotection[9]. Furthermore, GW-5074 exhibits a complex pharmacology as an allosteric glutamate dehydrogenase inhibitor[10] and an anti-polio virus (but not anti-Sendai virus) agent with a Raf1-independent mechanism of action[11]. Although neuroprotection by LRRK2 inhibition has been consistently shown in rodent models, similar effect in a human neuronal model has yet to be demonstrated. Recently, a selective LRRK2 inhibitor, LRRK2-IN-1, has been described, but it is unknown whether it blocks mutant LRRK2-induced toxicity in primary neurons[12]. Here we report the chemoproteomics-driven discovery of the first potent, selective LRRK2 inhibitors that attenuate toxicity in primary rodent and human neurons that is triggered by expression of mutant LRRK2.

To identify selective LRRK2 inhibitors binding to endogenous LRRK2 in tissue extracts, we adapted a chemical proteomics strategy previously used for target discovery and mechanism of action studies[13-15], so that precise IC_{50} measurements could be obtained to support a drug discovery project[16]. To this end, we made a linkable analog of the ATP-competitive non-selective kinase inhibitor sunitinib (la-sunitinib; **Fig. 1a** and **Synthetic Procedures in SI Text**) and immobilized it on a solid phase matrix[6, 13]. Under close to physiological conditions, this affinity matrix captured LRRK2 from mouse brain and kidney extracts (**Fig. 1b**). Binding and detection were specific, as no LRRK2-immunoreactive band was captured when tissue extracts from LRRK2 knock-out mice or when ethanolamine-derivatized matrix was utilized (**Fig. 1b** and **Fig. S1a, b**). To find a suitable lysate source for chemoproteomics-based screening against endogenous LRRK2 (**Fig. S2**), we profiled several tissues and human cell lines. We identified higher levels of LRRK2 in kidney than brain and observed expression of the kinase in heart, placenta, K562 and Ramos cells, but not in Jurkat, Molt-4, HL-60 or HeLa cells (**Fig. 1c** and **Fig. S1c**). This expression pattern is consistent with previously reported LRRK2 expression in human B (but not T) lymphocytes[17] and highlights the need for potent, selective LRRK2 chemical probes to interrogate its function in multiple tissues. To determine the IC_{50} for LRRK2 and many other kinases simultaneously, aliquots of mouse brain and kidney extracts were treated with various concentrations of a test compound, here sunitinib, or DMSO and were subsequently incubated with the la-sunitinib matrix. Proteins not blocked by free test compound were captured from the respective samples and quantified by chemical labeling of tryptic peptides with isobaric TMT™ tags, followed by tandem mass spectrometry analysis (LC-MS/MS) of

the combined peptide pools[16]. For identified protein targets, dose-response curves and IC_{50}s were computed from the decrease of reporter ion signals relative to the DMSO control (**Fig. S2, Table S1** and **SI Data Set**). Sunitinib displayed a sub-μM IC_{50} in this assay (**Fig. 1d**), but signal-to-background ratios obtained with this matrix in a dot-blot screening assay was too low. We therefore generated a series of sunitinib analogs and tested their ability to prevent binding of mouse brain LRRK2 to the la-sunitinib matrix (**Fig. S3**). Synthesis of a linkable analog of S7 (la-S7), one of the most effective compounds, was successful (**Fig. 1a, d** and **Synthetic Procedures in SI Text**). The la-S7 probe matrix improved the signal-to-background ratio (S/B > 5) of the dot blot array assay and enabled screening of a kinase-focused library of 127 compounds against mouse kidney lysate. One diaminopyrimidine screening hit (**Fig. 1e**), when tested at 3 μM, inhibited binding of mouse LRRK2 to la-S7 matrix by 90% and displayed an IC_{50} of 0.19 μM. It was further optimized by using the la-S7 matrix-based dot blot array for potency measurement and the quantitative LC-MS/MS-based assay for selectivity profiling. The lead compounds CZC-25146 and CZC-54252 resulted from this process (**Fig. 1e** and **Synthetic Procedures in SI Text**).

Both leads are potent (IC_{50} ~ 10-30 nM) inhibitors of binding of mouse LRRK2 to la-S7 matrix in the chemoproteomics assay (**Table S3** and **SI Data Set**). Furthermore, they also inhibited activity of recombinant human wild type LRRK2 enzyme (IC_{50} ~ 1-5 nM) and of the G2019S mutant (IC_{50} ~ 2-7 nM) with low nanomolar potency, as assessed by a time-resolved fluorescence resonance energy transfer assay (**Fig. 2a, b**). In contrast, GW-5074 was 30- to 100-fold less potent in this assay (**Fig. S4a**). Surprisingly, GW-5074 displayed very low potency in the la-S7 binding assay. Only incomplete dose-response curves and no valid IC_{50}s were obtained when concentrations as high as 100 μM were tested against both mouse kidney and human K562 extracts (**Fig. S4b**), suggesting that species differences are not the reason for this discrepancy. Possibly the lack of potency of GW-5074 in a high protein assay (5 mg/mL protein per data point) can be attributed to the compound's noted lack of selectivity and multiple binding modes resulting in low free concentrations available for LRRK2 binding.

High selectivity, particularly against neuronal kinases, was a key objective of this study. Consequently, we profiled the selectivity of CZC-25146 and CZC-54252 against mouse brain, human HeLa and mixed human Jurkat and Ramos cell extracts by quantitative LC-MS/MS utilizing la-S7 matrix or an established affinity matrix that contains seven immobilized non-selective compounds (“Kinobeads”) and therefore provides a comprehensive coverage of the kinome[13]. We determined IC_{50}s (assay range 10 nM to 2 μM) for 184 different protein kinases and one lipid kinase. Whereas the 4-chlorodiaminopyrimidine CZC-54252 exhibited good selectivity and potently inhibited binding of only ten human or mouse kinases, the 4-fluoro-diaminopyrimidine CZC-25146 displayed a very clean profile (**Fig. 2c** and **SI Data Set**). It inhibited only five kinases (PLK4, GAK, TNK1, CAMKK2 and PIP4K2C) with high potency, none of which have been classified as predictors of genotoxicity or hematopoietic toxicity[18, 19]. Furthermore, CZC-25146 neither caused cytotoxicity in human cortical neurons at concentrations below 5 μM over a seven-day treatment in culture (Fig. S5) nor did it block neuronal development (assessed as average neurite length or number of branchpoints) *in-vitro* (Fig. 3 and 4). Follow-up studies revealed that CZC-25146 possesses favorable pharmacokinetic properties, such as a volume of distribution of 5.4 L/kg and a clearance of 2.3 L/hr/kg (**Table S4**) that render it suitable for *in-vivo* studies.

Next, we addressed the question of whether selective LRRK2 inhibition protects against mutant LRRK2-induced neuronal toxicity to a similar extent as non-selective inhibition with GW-5074 did in an earlier study[7]. Since both CZC-25146 and CZC-54252 displayed poor brain penetration (~4 %) in our pharmacokinetics studies, we turned to *in vitro* models to

address this question. Towards this end, we overexpressed G2019S LRRK2 and R1441C LRRK2 in primary rodent cortical neurons. Both LRRK2 mutants caused cell injury, as assessed by neurite retraction and overt rounding up of the cells (**Fig. 3a, b**). Moreover, mutant LRRK2 triggered neuronal death, as assessed in a TUNEL assay measuring DNA fragmentation (**Fig. 3c**). In contrast, overexpression of eGFP or the kinase-dead double mutant G2019S/D1994A inflicted neither neuronal injury nor death, thus corroborating earlier studies[7, 20, 21](**Fig. 3a-c**). The most selective LRRK2 inhibitor, CZC-25146, attenuated G2019S LRRK2-induced neuronal injury and death in a concentration-dependent manner with an EC_{50} of ~ 100 nM. It completely blocked G2019S LRRK2 and R1441C-induced toxicity at higher concentrations (**Fig. 3d-e**), suggesting that inhibition of LRRK2 was sufficient for full neuroprotection *in-vitro*. Since the efficacy of a LRRK2 inhibitor had never been investigated in a human model of mutant LRRK2-induced toxicity before, we established a neurite morphology assay using primary human cortical neurons[22]. We transfected cultured cells with GFP and either WT or mutant LRRK2, and subsequently measured average neurite length and branchpoint counts by computer-aided morphometry (**Fig. 4a**). Similar to rodent neurons (**Fig. 3a-c**), overexpression of G2019S or R1441C mutant LRRK2 in human neurons resulted in cell injury, as assessed by a significant decrease in average neurite length. Kinase activity was required for this detrimental effect, since the kinase-deficient K1906M LRRK2 as well as the G2019S/K1906M and R1441C/K1906M double mutants showed no toxicity (**Fig. 4b**). Lack of toxicity observed with the latter mutant confirms the notion that even in LRRK2 protein carrying a mutation in the Roc domain, it is the kinase domain that controls toxicity and overall function[2]. G2019S LRRK2-induced human neuronal injury was attenuated by CZC-25146 with an EC_{50} of ~4 nM (EC_{50} CZC-54252 ~1 nM) and fully reversed to wild-type levels by both compounds at concentrations as low as 8 nM (1.6 nM for CZC-54252) (**Fig. 4c-d**). In human cortical neurons, no overt cytotoxicity was seen in the efficacious concentration range (only at 5 μM for CZC-25146 and ≥1 μM for CZC-54252) (**Fig. S5**).

In summary, we have developed a potent, selective, cell-penetrant and metabolically stable LRRK2 lead compound. Employing this small molecule inhibitor in the first study conducted to date in cultured primary human neurons, we have demonstrated that LRRK2 inhibition potently attenuates degeneration of human neurons induced by the mutant enzyme *in-vitro*.

This key result of our study suggests that selective inhibition of LRRK2 is sufficient for the neuroprotective effect observed in earlier studies with non-selective inhibitors such as GW-5074[7]. Cell culture and *in-vivo* studies performed with non-selective inhibitors are notoriously difficult to interpret: It is hardly feasible to test all possible mechanisms of action of a non-selective inhibitor, in case of GW-5074 Raf1-, B-Raf-[9] and allosteric glutamate dehydrogenase inhibition[10] and likely others[11]. Lee et al.[7] utilized another commercially available Raf1 inhibitor, ZM336372, to address the question of whether or not the mechanism of GW-5074 neuroprotection involved Raf1 kinase. ZM336372, however, is not a potent B-Raf inhibitor and its function in cells has been debated[23, 24]. Use of our selective LRRK2 inhibitor resolves this dilemma and suggests that selective LRRK2 inhibition could indeed be a promising new paradigm for Parkinson's disease therapy. Furthermore, compounds such as CZC-25146 will enable precise molecular studies of LRRK2 signaling and toxicity *in-vitro.*

It has been noted that LRRK2 expression is not restricted to medium-sized spiny striatal neurons, the key targets of the dopamine innervation. It is even more highly expressed in adult rat kidney and spleen[25], but little is known about the function of wild type or mutant LRRK2 in these organs. A recent genomic study implicated the LRRK2 gene locus in the genetic susceptibility to Crohn's disease, a chronic inflammatory disease of the gut[26].

LRRK2 expression is increased in inflamed intestinal tissue in Crohn's disease and the kinase may be involved in the production of reactive oxygen species during phagocytosis[27]. Analysis of functional consequences of LRRK2 inhibition in organs like kidney or blood with a precise and metabolically stable tool such as CZC-25146 will be of key importance for safety pharmacology *in-vitro* and *in-vivo* and thus for future drug discovery. Availability of selective, brain-impenetrant inhibitors may also prompt the in-depth investigation of possible therapeutic effects of selective LRRK2 inhibition in models of inflammatory disease in peripheral tissues *in-vivo.*

Quantitative mass spectrometry-based chemical proteomics has been used effectively in the past for target identification, compound re-profiling, and mechanism of action studies[13-15]. Conceptually expanding this approach, with the successful development of this potent and selective LRRK2 inhibitor, we have demonstrated that quantitative chemoproteomics with targeted mass spectrometric analysis[14, 16, 28, 29] can generate IC_{50} data that is robust. Our approach permits an understanding of structure-activity relationships that propels medicinal chemistry and provides a robust novel platform for lead optimization.

Methods

Screen for LRRK2 binding compounds

Screening in a competition-binding format was performed as previously described[14], with additional details provided in SI text.

Quantitative LC-MS/MS profiling of compounds

All profiling experiments were conducted as previously described[14, 15] with additional details in SI Text. PRIDE database (http://www.ebi.ac.uk/pride): mass spectrometry data set accession numbers 0000-0000. (submission codes in preparation).

Primary rat cortical neuronal culture, neuronal viability and TUNEL assays

Primary cortical neuronal cultures were prepared from gestational day 15 fetal rats as previously described [30]. Additional details are provided in SI text.

Primary human neuronal culture and neuronal health assay

Brain tissues from human fetuses ($n = 5$), ranging from 12 to 14 gestational weeks, were obtained through local agencies following all US federal guidelines on fetal tissue research. Cerebral cortices were collected in oxygenized Hank's balanced saline solution (HBSS) with an average postmortem delay of 15min and transported on ice. All procedures were performed under sterile conditions. The cortex was first triturated in Hank's balanced saline solution (HBSS), then filtered through a cell strainer and treated with 0.05 % Trypsin. After neutralization with 10 % FBS, the dissociated cells were resuspended in MEM supplemented with B-27 (Invitrogen), and plated in poly-D-lysine coated plates at a density of 2.5×10^4/well. Rat cortical cultures were prepared similarly from embryonic day 18 (E18) fetal rats. All cultures were maintained in MEM/2 % B-27/2 mM L-glutamine, with medium exchanged twice weekly. For characterization of LRRK2-induced neurite morphology change, various LRRK2 constructs and pmaxGFP (Amaxa) were co-transfected into neurons (20:1 ratio) with NeuroFECT (Genlantis) at DIV 14. To measure inhibitor effect, LRRK2 inhibitors or DMSO were also added at the indicated concentrations. The medium was exchanged on DIV17 with inhibitors replenished. On DIV 20, the cultures were harvested by fixation with 4% paraformaldehyde (PFA). Subsequent image acquisition and analysis were conducted on an ArrayScan VTI (Thermo Fisher Scientific) using the NeuronalProfiling V3.5 bioapplication. To monitor potential compound-mediated cytotoxicity, neuronal cultures were treated with inhibitors as described and tested in an AlamarBlue assay on DIV

20. Briefly, cells were incubated in 10 % AlamarBlue (AbD Serotec) in MEM for 2 h before fluorescent signals could be measured on a Gemini plate reader (Molecular Devices). DMSO-treated wells were employed as control on each plate for data normalization.

Supplementary Material

Refer to Web version on PubMed Central for supplementary material.

Acknowledgments

We are grateful to Melanie Jundt, Mareen Löttgers, Stepanie Melchert, Bea Kröh, Tatjana Rudi, Manuela Klös-Hudak, Julia-Irina Huber and Kira Weis for expert technical assistance, to David Simmons for comments on the manuscript, and to Frank Weisbrodt for help with the figures. We would like to thank Tim Edwards for support.

References

1. Gasser T. Molecular pathogenesis of Parkinson disease: insights from genetic studies. Expert Rev Mol Med. 2009; 11:e22. [PubMed: 19631006]
2. Cookson MR. The role of leucine-rich repeat kinase 2 (LRRK2) in Parkinson's disease. Nat Rev Neurosci. 2010; 11(12):791–7. [PubMed: 21088684]
3. Anand VS, Braithwaite SP. LRRK2 in Parkinson's disease: biochemical functions. Febs J. 2009; 276(22):6428–35. [PubMed: 19804416]
4. Lin X, Parisiadou L, Gu XL, Wang L, Shim H, Sun L, Xie C, Long CX, Yang WJ, Ding J, Chen ZZ, Gallant PE, Tao-Cheng JH, Rudow G, Troncoso JC, Liu Z, Li Z, Cai H. Leucine-rich repeat kinase 2 regulates the progression of neuropathology induced by Parkinson's-disease-related mutant alpha-synuclein. Neuron. 2009; 64(6):807–27. [PubMed: 20064389]
5. Anand VS, Reichling LJ, Lipinski K, Stochaj W, Duan W, Kelleher K, Pungaliya P, Brown EL, Reinhart PH, Somberg R, Hirst WD, Riddle SM, Braithwaite SP. Investigation of leucine-rich repeat kinase 2 : enzymological properties and novel assays. Febs J. 2009; 276(2):466–78. [PubMed: 19076219]
6. Drewes, G.; Hopf, C.; Reader, V. METHODS FOR THE IDENTIFICATION OF LRRK2 INTERACTING MOLECULES AND FOR THE PURIFICATION OF LRRK2.. 2009. Patent No. US2009220992
7. Lee BD, Shin JH, Vankampen J, Petrucelli L, West AB, Ko HS, Lee YI, Maguire-Zeiss KA, Bowers WJ, Federoff HJ, Dawson VL, Dawson TM. Inhibitors of leucine-rich repeat kinase-2 protect against models of Parkinson's disease. Nat Med. 2010
8. Liu M, Dobson B, Glicksman MA, Yue Z, Stein RL. Kinetic mechanistic studies of wild-type leucine-rich repeat kinase 2: characterization of the kinase and GTPase activities. Biochemistry. 2010; 49(9):2008–17. [PubMed: 20146535]
9. Chen HM, Wang L, D'Mello SR. Inhibition of ATF-3 expression by B-Raf mediates the neuroprotective action of GW5074. J Neurochem. 2008; 105(4):1300–12. [PubMed: 18194435]
10. Li M, Smith CJ, Walker MT, Smith TJ. Novel inhibitors complexed with glutamate dehydrogenase: allosteric regulation by control of protein dynamics. J Biol Chem. 2009; 284(34): 22988–3000. [PubMed: 19531491]
11. Arita M, Wakita T, Shimizu H. Characterization of pharmacologically active compounds that inhibit poliovirus and enterovirus 71 infectivity. J Gen Virol. 2008; 89(Pt 10):2518–30. [PubMed: 18796721]
12. Deng X, Dzamko N, Prescott A, Davies P, Liu Q, Yang Q, Lee JD, Patricelli MP, Nomanbhoy TK, Alessi DR, Gray NS. Characterization of a selective inhibitor of the Parkinson's disease kinase LRRK2. Nat Chem Biol. 2011; 7(4):203–5. [PubMed: 21378983]
13. Bantscheff M, Eberhard D, Abraham Y, Bastuck S, Boesche M, Hobson S, Mathieson T, Perrin J, Raida M, Rau C, Reader V, Sweetman G, Bauer A, Bouwmeester T, Hopf C, Kruse U, Neubauer G, Ramsden N, Rick J, Kuster B, Drewes G. Quantitative chemical proteomics reveals mechanisms of action of clinical ABL kinase inhibitors. Nat Biotechnol. 2007; 25(9):1035–44. [PubMed: 17721511]

14. Bantscheff M, Hopf C, Savitski MM, Dittmann A, Grandi P, Michon AM, Schlegl J, Abraham Y, Becher I, Bergamini G, Boesche M, Delling M, Dumpelfeld B, Eberhard D, Huthmacher C, Mathieson T, Poeckel D, Reader V, Strunk K, Sweetman G, Kruse U, Neubauer G, Ramsden NG, Drewes G. Chemoproteomics profiling of HDAC inhibitors reveals selective targeting of HDAC complexes. Nat Biotechnol. 2011; 29(3):255–65. [PubMed: 21258344]
15. Kruse U, Pallasch CP, Bantscheff M, Eberhard D, Frenzel L, Ghidelli S, Maier SK, Werner T, Wendtner CM, Drewes G. Chemoproteomics-based kinome profiling and target deconvolution of clinical multi-kinase inhibitors in primary chronic lymphocytic leukemia cells. Leukemia. 2010; 25(1):89–100. [PubMed: 20944678]
16. Savitski MM, Fischer F, Mathieson T, Sweetman G, Lang M, Bantscheff M. Targeted Data Acquisition for Improved Reproducibility and Robustness of Proteomic Mass Spectrometry Assays. J Am Soc Mass Spectrom. 2010
17. Maekawa T, Kubo M, Yokoyama I, Ohta E, Obata F. Age-dependent and cell-population-restricted LRRK2 expression in normal mouse spleen. Biochem Biophys Res Commun. 2010; 392(3):431–5. [PubMed: 20079710]
18. Olaharski AJ, Gonzaludo N, Bitter H, Goldstein D, Kirchner S, Uppal H, Kolaja K. Identification of a kinase profile that predicts chromosome damage induced by small molecule kinase inhibitors. PLoS Comput Biol. 2009; 5(7):e1000446. [PubMed: 19629159]
19. Olaharski AJ, Bitter H, Gonzaludo N, Kondru R, Goldstein DM, Zabka TS, Lin H, Singer T, Kolaja K. Modeling bone marrow toxicity using kinase structural motifs and the inhibition profiles of small molecular kinase inhibitors. Toxicol Sci. 2010; 118(1):266–75. [PubMed: 20810542]
20. Smith WW, Pei Z, Jiang H, Dawson VL, Dawson TM, Ross CA. Kinase activity of mutant LRRK2 mediates neuronal toxicity. Nat Neurosci. 2006; 9(10):1231–3. [PubMed: 16980962]
21. Smith WW, Pei Z, Jiang H, Moore DJ, Liang Y, West AB, Dawson VL, Dawson TM, Ross CA. Leucine-rich repeat kinase 2 (LRRK2) interacts with parkin, and mutant LRRK2 induces neuronal degeneration. Proc Natl Acad Sci U S A. 2005; 102(51):18676–81. [PubMed: 16352719]
22. MacLeod D, Dowman J, Hammond R, Leete T, Inoue K, Abeliovich A. The familial Parkinsonism gene LRRK2 regulates neurite process morphology. Neuron. 2006; 52(4):587–93. [PubMed: 17114044]
23. Hall-Jackson CA, Eyers PA, Cohen P, Goedert M, Boyle FT, Hewitt N, Plant H, Hedge P. Paradoxical activation of Raf by a novel Raf inhibitor. Chem Biol. 1999; 6(8):559–68. [PubMed: 10421767]
24. Van Gompel JJ, Kunnimalaiyaan M, Holen K, Chen H. ZM336372, a Raf-1 activator, suppresses growth and neuroendocrine hormone levels in carcinoid tumor cells. Mol Cancer Ther. 2005; 4(6): 910–7. [PubMed: 15956248]
25. Westerlund M, Belin AC, Anvret A, Bickford P, Olson L, Galter D. Developmental regulation of leucine-rich repeat kinase 1 and 2 expression in the brain and other rodent and human organs: Implications for Parkinson's disease. Neuroscience. 2008; 152(2):429–36. [PubMed: 18272292]
26. Van Limbergen J, Wilson DC, Satsangi J. The genetics of Crohn's disease. Annu Rev Genomics Hum Genet. 2009; 10:89–116. [PubMed: 19453248]
27. Gardet A, Benita Y, Li C, Sands BE, Ballester I, Stevens C, Korzenik JR, Rioux JD, Daly MJ, Xavier RJ, Podolsky DK. LRRK2 is involved in the IFN-gamma response and host response to pathogens. J Immunol. 2010; 185(9):5577–85. [PubMed: 20921534]
28. Pan S, Aebersold R, Chen R, Rush J, Goodlett DR, McIntosh MW, Zhang J, Brentnall TA. Mass spectrometry based targeted protein quantification: methods and applications. J Proteome Res. 2009; 8(2):787–97. [PubMed: 19105742]
29. Sharma K, Weber C, Bairlein M, Greff Z, Keri G, Cox J, Olsen JV, Daub H. Proteomics strategy for quantitative protein interaction profiling in cell extracts. Nat Methods. 2009; 6(10):741–4. [PubMed: 19749761]
30. West AB, Moore DJ, Biskup S, Bugayenko A, Smith WW, Ross CA, Dawson VL, Dawson TM. Parkinson's disease-associated mutations in leucine-rich repeat kinase 2 augment kinase activity. Proc Natl Acad Sci U S A. 2005; 102(46):16842–7. [PubMed: 16269541]

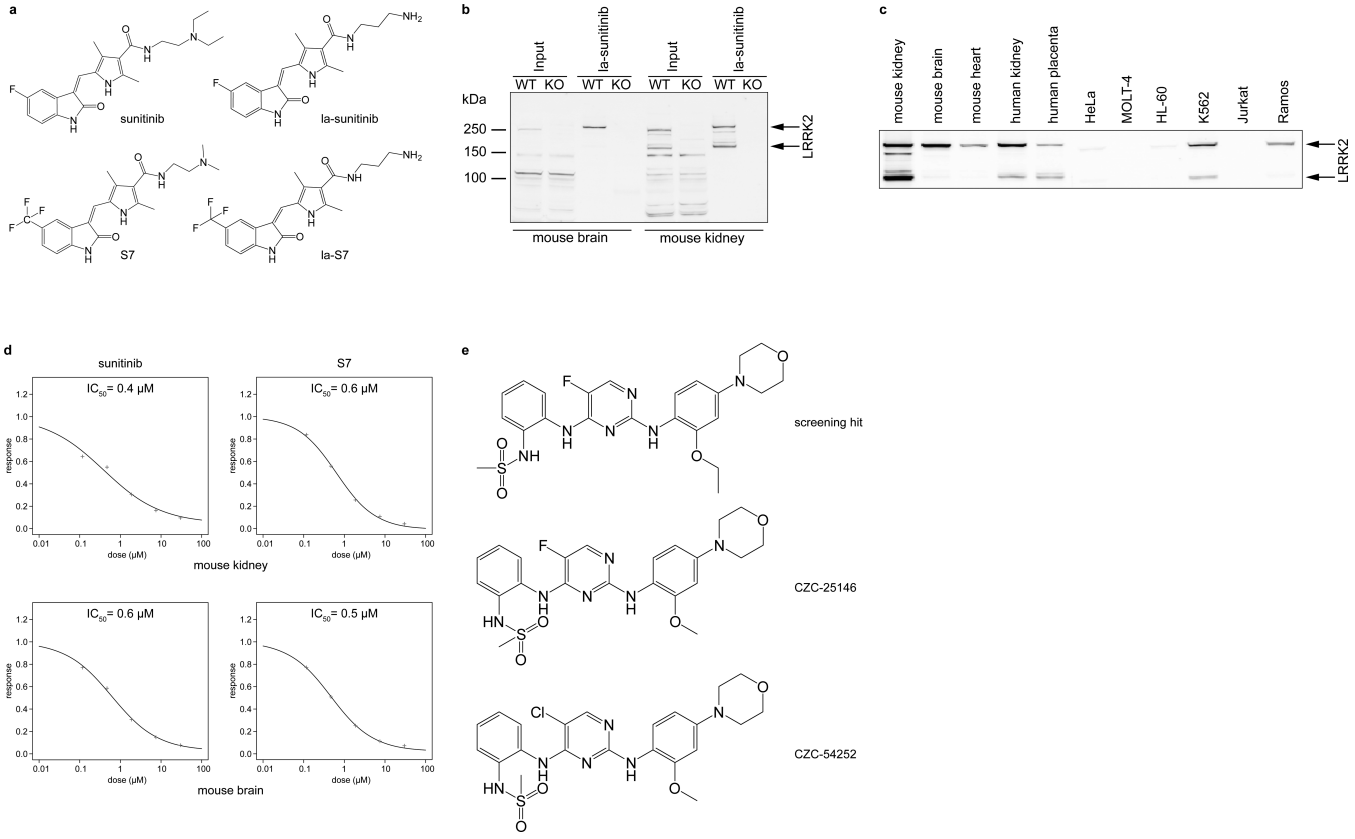

Figure 1. Chemoproteomics-based discovery of LRRK2 lead compounds

a) Structures of sunitinib, a linkable analog (la) of sunitinib, the optimized sunitinib analog S7 and a linkable derivative thereof.

b) la-sunitinib matrix specifically captures LRRK2 from mouse brain and kidney extracts (Input). Affinity matrix was incubated with detergent extract (5 mg) from brain or kidney of wild type (WT) or LRRK2 knock-out (KO) mice. Bound proteins were eluted with SDS sample buffer and probed with anti-LRRK2 antibody. Peptide sequence coverage observed by LC-MS/MS (**Fig. S1d, Table S2** and **SI Data Set 1**) suggests that the lower band seen in kidney extract represents an N-terminally truncated fragment of LRRK2. Molecular weights markers of 250 kDa, 150 kDa and 100 kDa are indicated.

c) la-sunitinib captures LRRK2 from various human and mouse cell and tissue sources. Proteins captured by probe matrix were analyzed by immunoblot with anti-LRRK2 antibody.

d) Sunitinib and the analog S7 are equipotent for LRRK2 in a chemoproteomics binding assay (**Fig. S2, S3**). Mouse kidney (upper panels) or mouse brain (lower panels) extracts (5 mg) were pre-incubated with 30 μM, 7.5 μM, 1.88 μM, 0.47 μM, 0.12 μM (or vehicle control) of free sunitinib (left panels) or S7 (right panels). Kinase targets not occupied by free test compounds were captured by la-sunitinib matrix. Proteins eluted from the matrix were quantified by chemical labeling of tryptic peptides with isobaric TMT tags, followed by tandem mass spectrometry analysis (LC-MS/MS) of the combined peptide pools. Concentration-response curves and IC_{50} for LRRK2 were computed from the changes of reporter ion signals relative to the DMSO control for all sequenced peptides corresponding to LRRK2. An S7-affinity matrix displayed an improved signal-to-noise ratio in a dot-blot array assay format (**Fig. S2, S3**) and was used for screening of 127 compounds against endogenous LRRK2 from mouse kidney.

e) Structures of the screening hit chosen for optimization and its analogs CZC-25146 and CZC-54252.

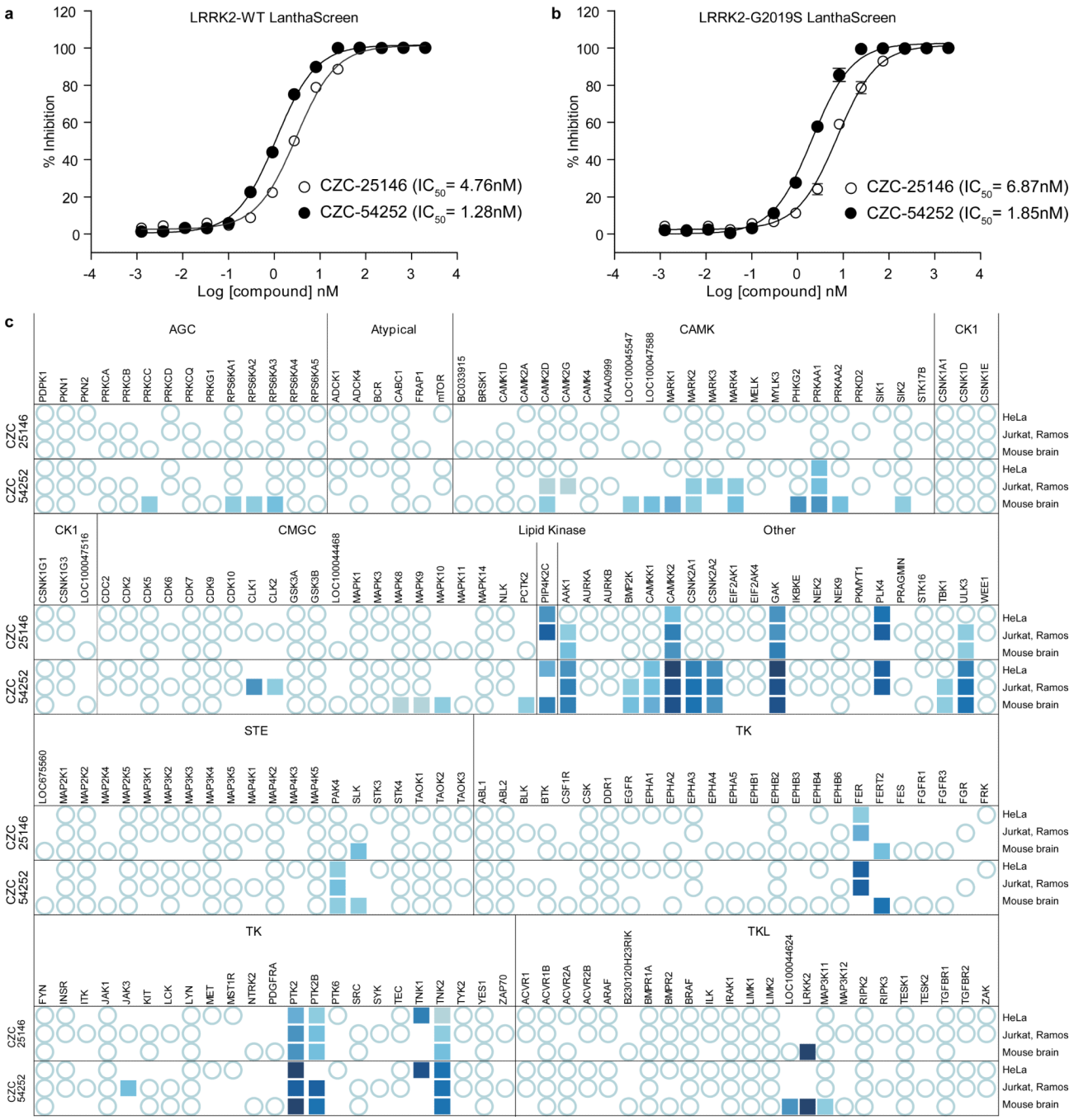

Figure 2. CZC-25146 and CZC-54252 are potent and selective LRRK2 inhibitors

a) b) CZC-25146 (open circles) and CZC-54252 (closed circles) are potent inhibitors of (a) human wild type LRRK2 (IC_{50} = 4.76 nM and 1.28 nM, respectively) and (b) G2019S LRRK2 activity (IC_{50} = 6.87 nM and 1.85 nM, respectively). IC_{50}s were determined in a time-resolved fluorescence resonance energy transfer (TR-FRET)-based kinase activity assay. The ATP concentration (100 μM) approximates the K_M of LRRK2 for ATP. Note that neither compound displayed a preference for the wild type or the mutant enzyme. **c)** CZC-25146 and CZC-54252 are LRRK2-selective, as assessed by quantitative mass spectrometry assay (**Fig. S2**). Concentration-response curves for each compound were

generated in three different lysates - HeLa, a Jurkat/Ramos mixture, and mouse brain -using Kinobeads matrix[13] (la-S7 matrix for LRRK2) as a kinase capturing tool. Bound proteins were quantified by LC-MS/MS (**SI Text**). pIC_{50}s are represented as a heat map: Kinases that were captured by Kinobeads matrix but not competed by compound are represented as open circles. Kinases whose binding to Kinobeads were affected by free test compound are indicated by filled squares. pIC_{50}s between 10 nM (dark blue) and 2 μM (light blue) were split into ten equal bins and color-coded. Kinases that were not captured from a given cell source are not marked.

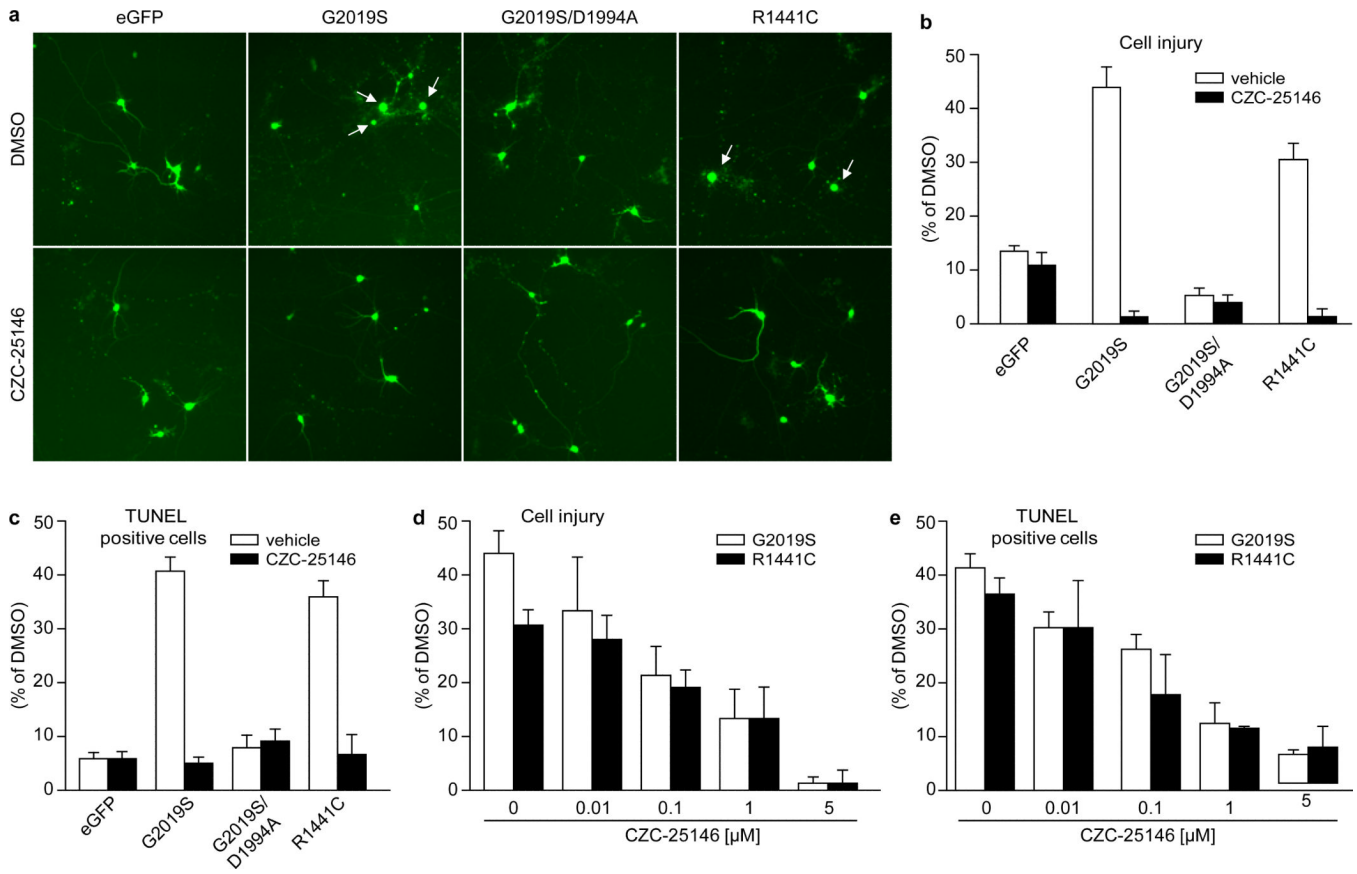

Figure 3. CZC-25146 potently attenuates mutant LRRK2-mediated toxicity in primary rodent neurons

LRRK2 and eGFP constructs were combined in a molar ratio of 15:1, respectively, and transfected by use of Lipofectamine 2000 (Invitrogen) at DIV (day *in vitro*) 14 into rat primary cortical neuronal cultures. CZC-25146 was administered at the time of transfection and continued until toxicity assessments. Cell injury was defined as loss of viable neurons, i.e. those neurons having at least one smooth extension (neurite) with twice the length of the cell body.

a) Representative photomicrographs of each experimental group. On DIV 16, images were collected on a Zeiss Automatic stage with Axiovision 6.0.

b) Quantification of cell injury induced by transfected LRRK2 and eGFP constructs, normalized to the number of viable neurons transfected with eGFP, in the presence of 1 μM CZC-25146 (closed bars) or DMSO as vehicle control (open bars). Viable neurons were defined as having at least one smooth extension (neurite) with twice the length of the cell body.

c) Quantification of the TUNEL assay, normalized to number of TUNEL positive neurons transfected with eGFP and LRRK2 in the presence of CZC-25146 (closed bars) or DMSO as vehicle control (open bars).

d) Quantification of cell injury of rat cortical neurons transfected with LRRK2 G2019S (open bars) or R1441C (closed bars), normalized to number of viable neurons transfected with eGFP, in the presence of various concentrations of CZC-25146.

e) Quantification of the TUNEL assay for neurons transfected with LRRK2 G2019S (open bars) or R1441C (closed bars), normalized to number of TUNEL-positive neurons transfected with eGFP, in the presence of various concentrations of CZC-25146.

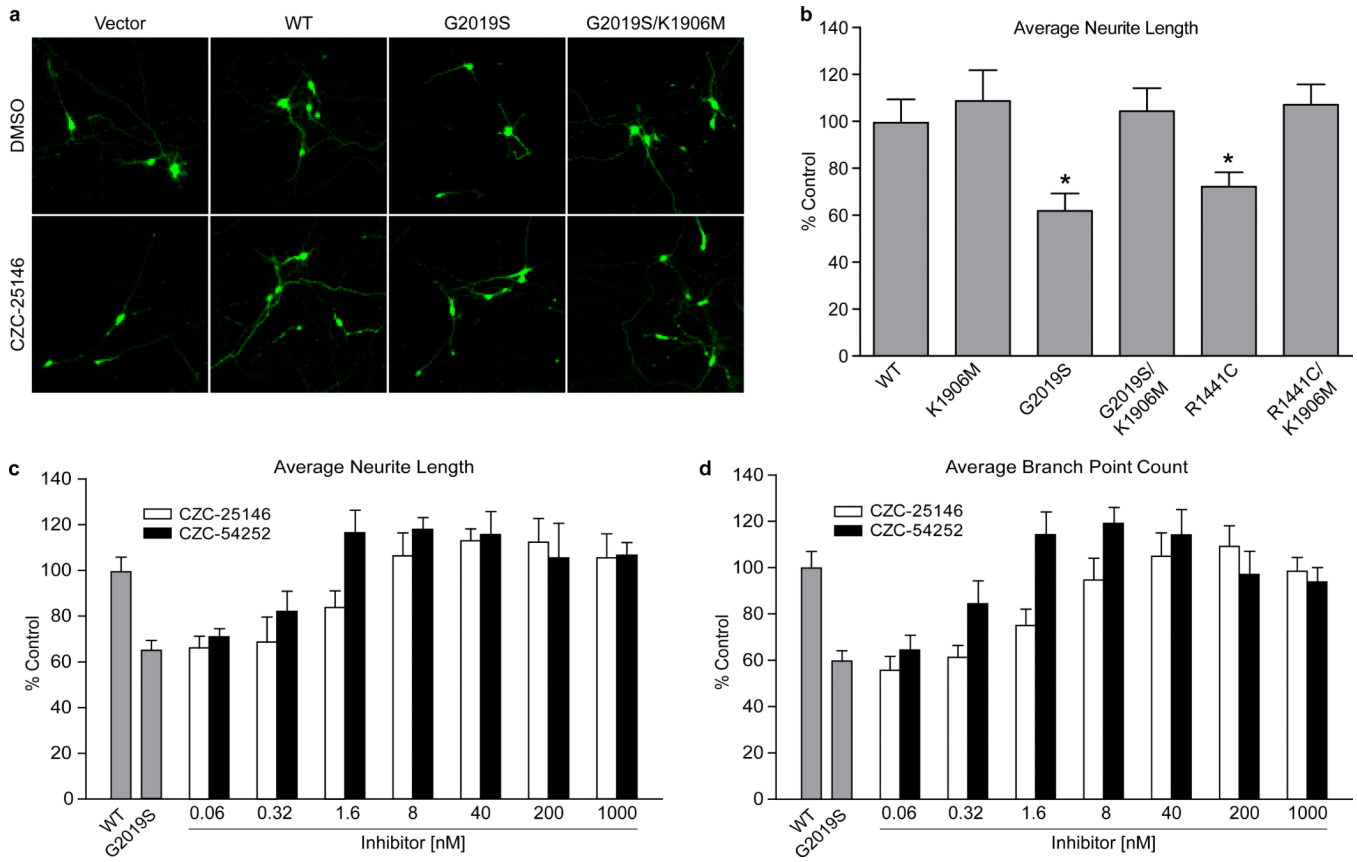

Figure 4. CZC-25146 and CZC-54252 potently attenuate mutant LRRK2-mediated toxicity in primary human neurons

a) Representative images of transfected human cortical neurons treated with either DMSO or CZC-25146 (40 nM). The neurons were transfected with various LRRK2 constructs as indicated or empty vectors, along with GFP for neurite tracing.

b) LRRK2 G2019S and R1441C mutants reduce the average neurite length in a kinase-dependent manner. Quantification was done with a computerized algorithm and the data were expressed as percentage of the empty vector control. * $p < 0.01$ versus control. Note that wild type LRRK2 and the kinase-deficient K1906M, R1441C/K1906M and G2019S/K1906M mutants did not cause a reduction in neurite length.

c) d) LRRK2 inhibitors, CZC-25146 and CZC-54252, rescue LRRK2 G2019S-induced neurite defects in a dose-dependent manner. LRRK2 G2019S-transfected neurons were treated with DMSO or LRRK2 inhibitors at the indicated concentrations. Quantification was done with a computerized algorithm and the data were expressed as percentage of the empty vector control. Note that the G2019S mutant decreased average neurite length and branch point counts, both of which were fully restored by LRRK2 inhibitor treatment with estimated EC_{50} values below 8 nM.